Chapter

Segmentation and Merging of Closed Water Bodies by Wind Waves

Takaaki Uda, Masumi Serizawa and Shiho Miyahara

Abstract

The segmentation and merging of elongated shallow water body with a large aspect ratio by wind waves were predicted using the Type 6 BG model. The deformation of a circular lake by wind waves was also studied when a straight seawall cutting a part of the water body was constructed in a lake for land reclamation, together with the investigation on the effect of the construction of detached breakwaters to the surrounding lakeshore. Finally, the formation of oriented lakes, groups of lake basins with a common long-axis orientation found in vast areas of the Arctic Coastal Plain, was predicted using the Type 6 BG model.

Keywords: segmentation, merging, elongated water body, wind waves, circular lake, detached breakwater, oriented lakes

1. Introduction

In a shallow water body, topographic changes may take place owing to wind waves. In the ordinary case, the wave incidence angle relative to the direction normal to the shoreline is small, but in a narrow water body with a large aspect ratio, it may exceed 45°, and the shoreline may become unstable owing to the mechanism of high-angle wave instability [1–3]. Cuspate forelands that develop from both shores of a narrow water body may connect with each other, resulting in the segmentation of the water body into smaller rounded lakes [4–6]. Typical examples can be seen in a water body facing the Chukchi Sea in Russia, as shown in **Figure 1** [7], where the sizes of the water bodies formed by the segmentation differ from each other depending on the size of the original water body. In **Figure 2**, an enlarged image of the rectangular area in **Figure 1**, another segmentation of the shallow lake can be seen, in which the lakeshore is at a primitive stage of development, and cuspate forelands alternately develop from both shores. Regarding these phenomena, the division and reduction of a fetch distance owing to the formation of a large shoreline protrusion and the resulting change in the wave field become key factors. Ashton et al. [1, 5] successfully modeled the development of shoreline irregularities into cuspate spits owing to the instability mechanism only using longshore sand transport formula. Serizawa et al. [8] also explained them by the numerical simulation using the BG model. In this study, 3D beach changes during the segmentation of a shallow water body into small lakes were first predicted using the Type 6 BG model [7, 9, 10] in Section 2.

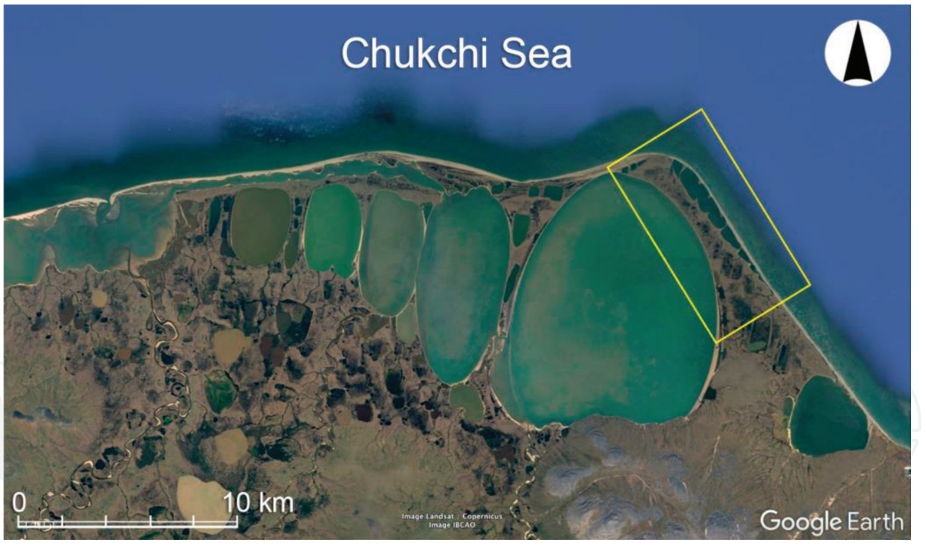

Figure 1.
Example of segmentation of a shallow water body facing the Chukchi Sea in Russia.

Figure 2.
*Enlarged image of rectangular area in **Figure 1**.*

The second case relates to the deformation of a circular lake. Because a circular lake is completely stable for the wind waves generated when wind blows from all directions with the same probability of occurrence and intensity, no lakeshore changes occur unless the landform changes are exerted, but when a seawall or detached breakwaters are constructed at part of the lake, the wave field will change, causing the lakeshore changes [11]. In Section 3, the deformation of a circular lake by wind waves was studied when a straight seawall cutting part of the water body was constructed in a lake, together with the investigation on the effect of the construction of detached breakwaters to the surrounding lakeshore in Section 4.

In vast areas of the Arctic Coastal Plain, oriented lakes, groups of lake basins with a common long-axis orientation, can be found [12]. Oriented lakes in permafrost regions were originally thermokarst features [13]. The shape of oriented lakes in North America is often elliptical with their long axis generally aligned in the N-NW direction, perpendicular to the direction of the prevailing summer winds. The initial cause of the formation of a thaw lake or depression may be the random melting of ground ice or subsidence of the ground followed by the accumulation of water in the depression. Mackay [14] developed a mathematical model that relates the lake shape with the resultant wind vectors and the square of the velocity and attempted to analyze the equilibrium forms of lakes that might be produced by winds of today. However, the precise mechanism of the lake orientation remained unexplained. So, the formative mechanism of oriented lakes was investigated using the Type 6 BG model in Section 5 [15].

2. Numerical simulation of 3D segmentation of elongated water body

2.1 Formation of alternate cuspate forelands in a lake

Lake Kitaura located in the Kanto Plains, Japan, is a shallow lagoon with a water area of 35.2 km^2 and 25 km length (**Figure 3**), which is surrounded by the Kashima and Namekata Tablelands with an elevation as low as 40 and 30 m, respectively. Wind, therefore, can blow over the surface of this shallow water body without significant sheltering effect by the local topographies. Referring the wind rose measured at the center of Lake Kasumigaura located 10 km west of Lake Kitaura, the predominant wind directions are NNE, N, and NE, which are close to the direction of the principal axis of Lake Kitaura, resulting in the generation of strong wind waves [7, 9, 10].

In **Figure 3**, many cuspate forelands alternately develop along both shores of the lake. Because the location of the cuspate forelands in the central part of the lagoon coincides with that of ridges extending toward the lake, it is assumed that no cuspate forelands have been formed owing to the shoreline instability, whereas

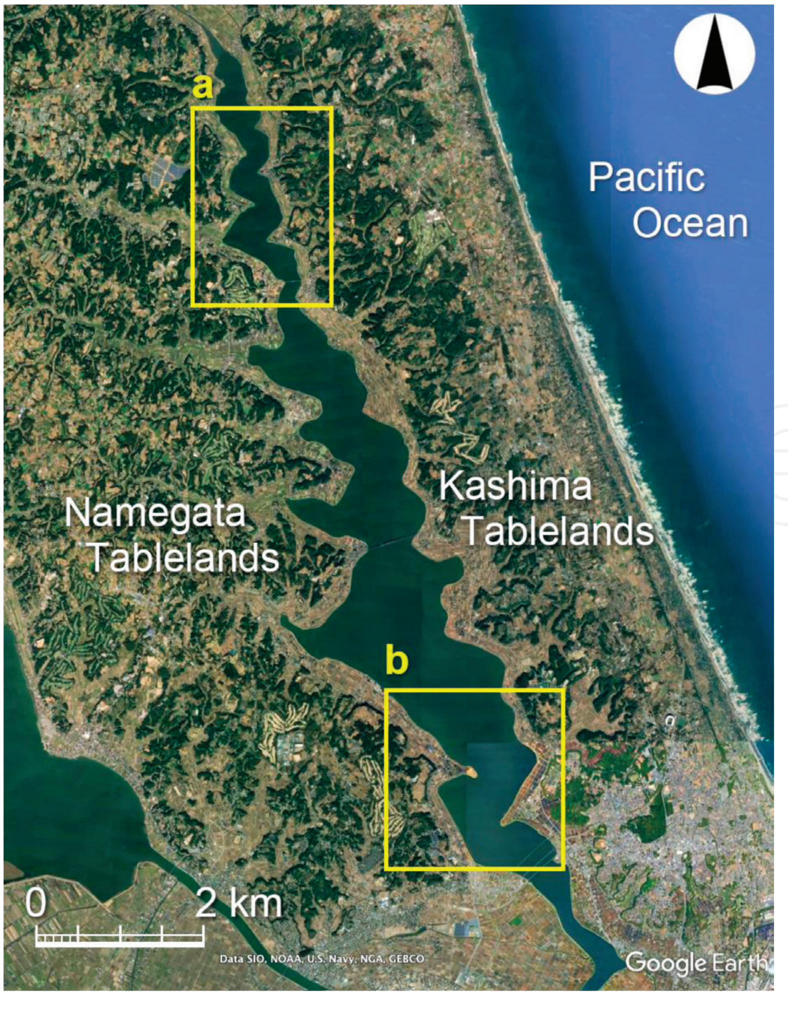

Figure 3.
Formation of alternate cuspate forelands in Lake Kitaura.

cuspate forelands develop independent of the location of the ridges in the northern and southern rectangular areas (**a** and **b**) shown in **Figure 3**. **Figure 4 (a** and **b**) show the enlarged aerial photographs of these areas. In these areas, the cuspate forelands alternately develop similarly to the example in a shallow lagoon facing the Chukchi Sea in Russia.

2.2 Calculation conditions

Consider a shallow water body with a flat, solid bed of 3 m depth. The lakeshore was assumed to have a berm of 1 m height and a uniform slope of 1/20. A random noise with an amplitude of ΔZ = 0.1 m was added to the slope between Z = −3 and 1 m in the initial profile. Assuming that the wind velocity was 20 m/s and wind blew from all the directions with the same probability and intensity, the wind direction at each step was randomly determined based on a probability distribution function. The depth distribution of longshore sand transport $\varepsilon(Z)$ was assumed to be uniform over the depth. **Table 1** summarizes the conditions for the calculation of the segmentation of a narrow water body.

2.3 Calculation results

Figure 5 shows the segmentation of a narrow slender water body of 4.5 km length and 0.64 km width (aspect ratio = 7) into small lakes. Sandbars with irregular shapes such as cuspate spits had started to develop along the shoreline after 5000 steps (**Figure 5(b)**). The protruded shoreline produced a wave-shelter zone downcoast, causing a decrease in longshore sand transport, whereas it increased at the tip of the protrusion. Thus, small-scale sandbars were absorbed into a larger sandbar, and the size of the sandbar increased by 1×10^4 steps (**Figure 5(c)**). These results explain the formative mechanism of alternate sandbars observed in the water bodies facing the Chukchi Sea and Lake Kitaura.

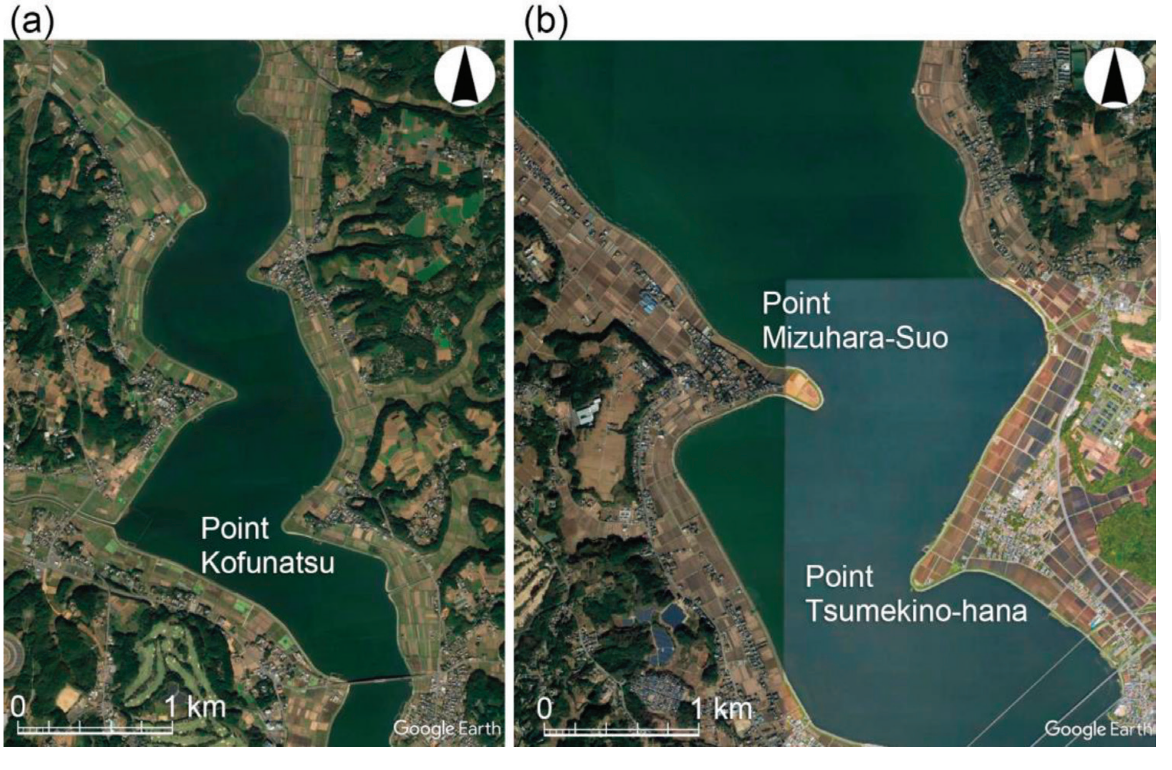

Figure 4.
Aerial photographs of the northern and southern parts, a and b, of Lake Kitaura.

By 2 × 10⁴ steps, the sandbars on both shores connected with each other result in the segmentation of the elongated water body into three smaller, elliptic lakes (**Figure 5(e)**). The segmentation continued with time, and the shape of the lake became rounded (**Figure 5(f)**). After 3×10^4 steps, the three lakes had started to become circular (**Figure 5(g)**), and the three rounded lakes were formed by 10^5 steps (**Figure 5(h)**). The segmentation of the elongated water body into three lakes was similar to that as in [5], but the 3D beach changes including the formation of sandbars with a hound's tooth pattern were possible to predict in this study.

Calculation method	Type 6 BG model
Wind velocity	20 m/s
Berm height h_R	1 m
Depth of closure h_c	3 m
Equilibrium slope tanβ_c	1/20
Coefficients of sand transport	Longshore and cross-shore sand transport coefficient K_s = 0.2
Mesh size	$\Delta x = \Delta y$ = 20 m
Time intervals	Δt = 10 h
Duration of calculation	10^6 h (10^5 steps)
Boundary conditions	Shoreward and landward ends q_x = 0 Right and left boundaries q_y = 0

Table 1.
Conditions for calculation of segmentation of a narrow water body.

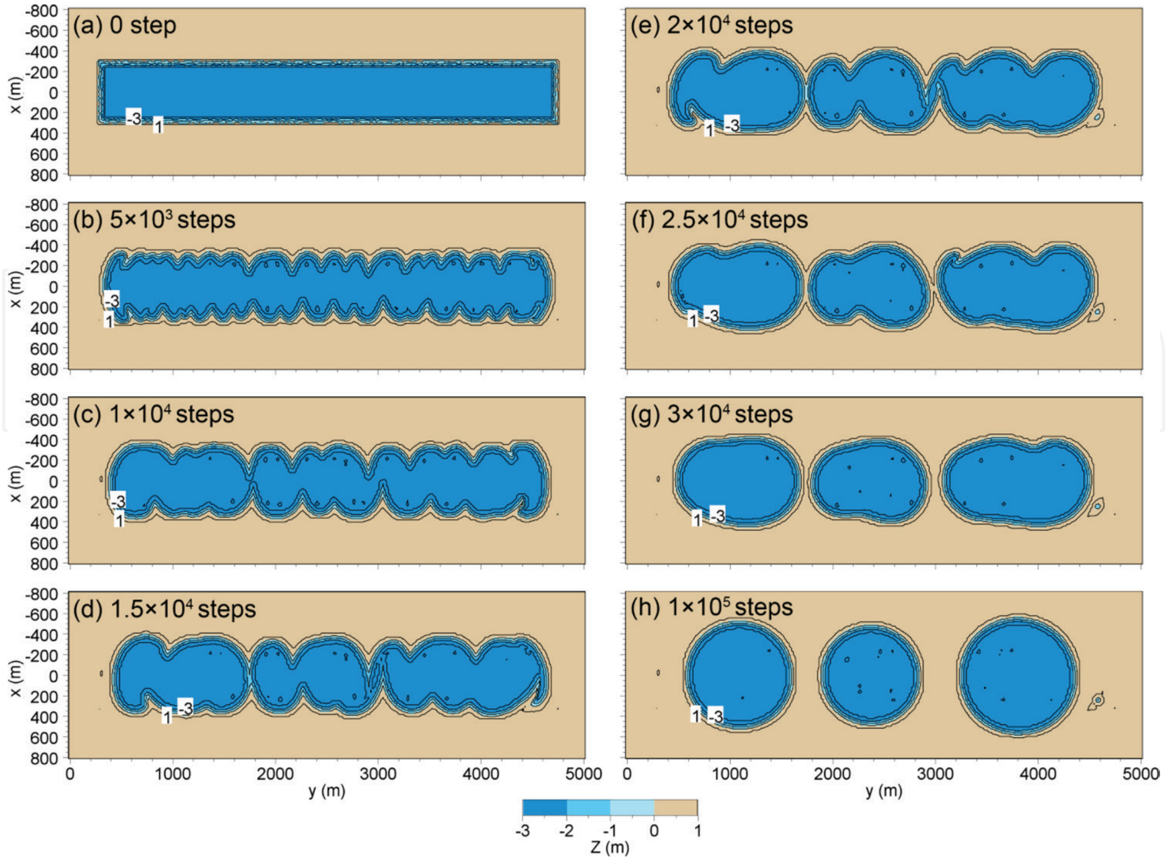

Figure 5.
Segmentation of a slender lake of 4.5 km length and 0.64 km width (aspect ratio = 7) into small lakes.

3. Effect of land reclamation and construction of detached breakwaters in a circular lake

3.1 Calculation conditions

A circular lake of 1.2 km radius was considered, and part of the circular lake was cut off by a seawall extending along $y = -600$ m to investigate the effect of the land reclamation on the nearby lakeshore [11], as shown in **Figure 6**. The depth of a circular water body was assumed to be 3 m, and a sandy beach with a berm height of 1 m and a uniform slope of 1/20 was set along the peripheral shoreline of a lake. Wind velocity was assumed to be 20 m/s, and wind blew from all directions with the same probability of occurrence and intensity in all cases. The wind direction in each step was set using random numbers. The depth distribution of sand transport was assumed to be given by a uniform distribution throughout the depth. **Table 2** summarizes the conditions for the calculation of deformation of a circular lake.

3.2 Calculation results

When a seawall was constructed in a part of the lake, the wave field changed, inducing the lakeshore changes, as shown in **Figure 6**. The shape of the lake was more rounded after 2×10^5 steps (**Figure 6(b)**) relative to the initial shape shown in **Figure 6(a)**. **Figure 7** shows the seabed difference after 2×10^5 steps with reference to the initial topography. Note that the shoreline receded on the opposite shore against the seawall after the construction of the seawall and the lake shape became more rounded. The mechanism of these lakeshore changes can be explained using a schematic diagram as illustrated in **Figure 8**.

Set points C on ark AB and C′ at a point where a straight line connecting point C with the center of the circular lake intersects the shoreline of the water body. Set the fetch distance between points C and C′ to be F1. Then, a straight line tangent to the circle is drawn at point C, and the fetch distance in each direction divided at the same angular intervals is drawn (**Figure 8**). The numbers 2–9 and 2′–9′ are located on the right and left half of the circular lake, respectively. When wind blows from

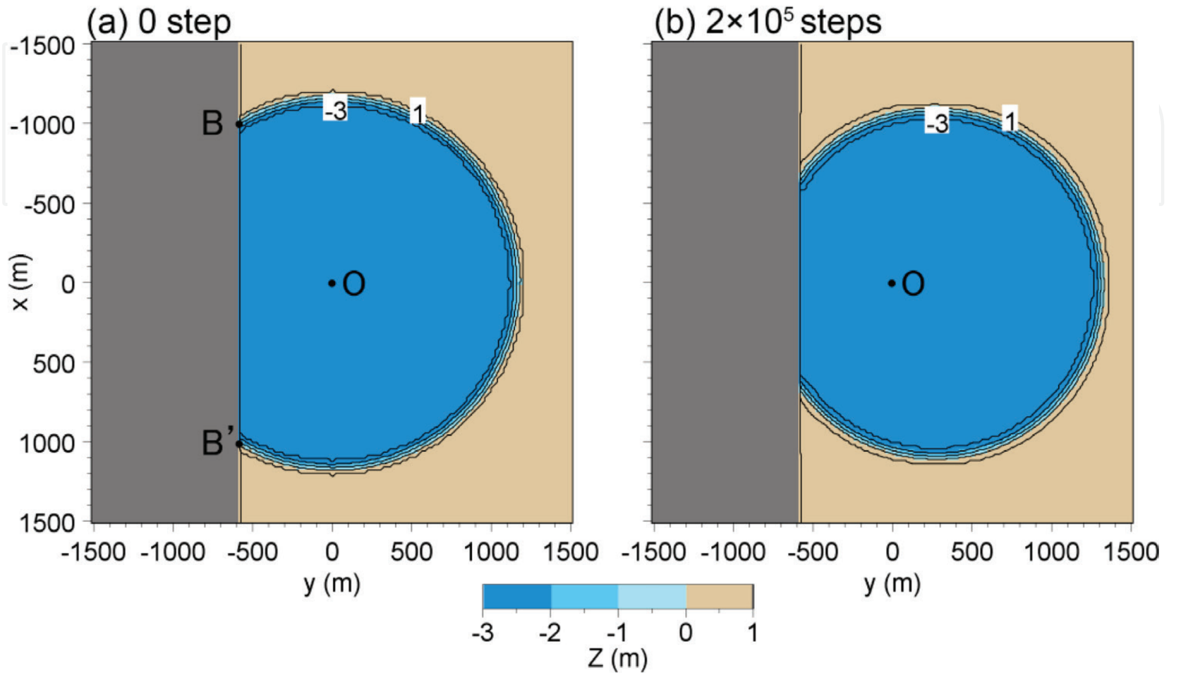

Figure 6.
Change in circular lake cut off by a straight seawall.

Calculation method	Type 6 BG model
Wind velocity	20 m/s
Berm height h_R	1 m
Depth of closure h_c	3 m
Equilibrium slope $\tan\beta_c$	1/20
Coefficients of sand transport	Longshore and cross-shore sand transport coefficient K_s = 0.2
Mesh size	$\Delta x = \Delta y = 20$ m
Time intervals	$\Delta t = 5$ h
Duration of calculation	10^6 h (2×10^5 steps)
Boundary conditions	Shoreward and landward ends $q_x = 0$ Right and left boundaries $q_y = 0$

Table 2.
Conditions for calculation of deformation of a circular lake.

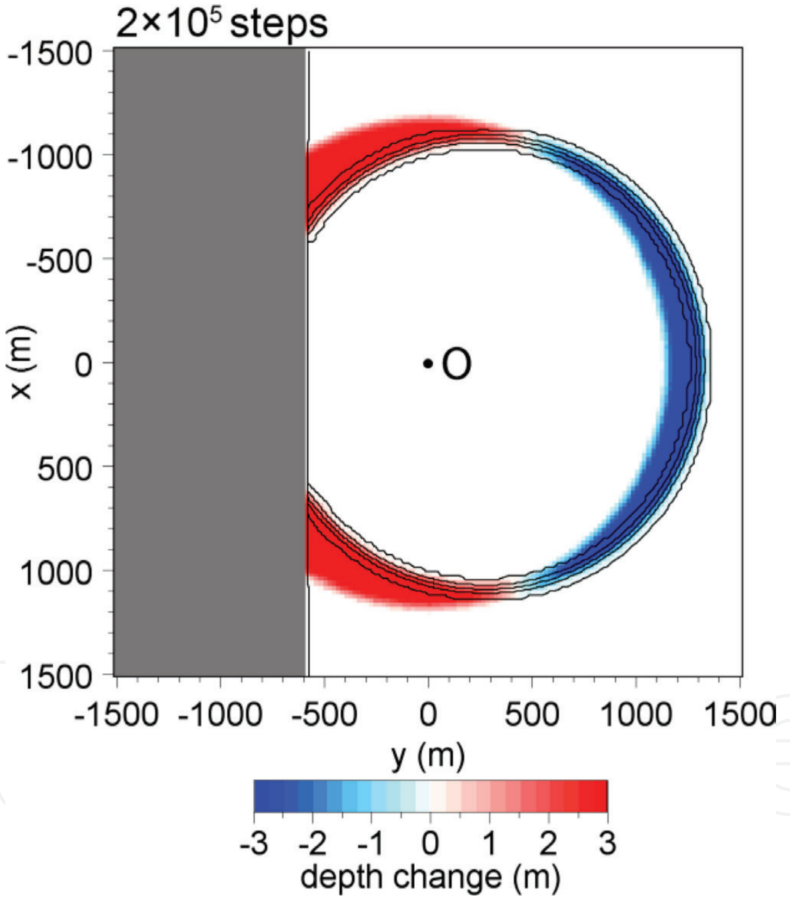

Figure 7.
Seabed differences after 2×10^5 steps with reference to initial topography.

the directions between fetch F2 and fetch F9, which extend radially, rightward longshore sand transport is generated with respect to the direction normal to the shoreline at point C, because wind waves are incident from the counterclockwise direction. In contrast, when wind blows from the directions between fetch F2' and fetch F9', leftward longshore sand transport is generated at point C. Longshore sand transport is 0 under the wave incidence from fetch F1 because of the wave incidence normal to the shoreline.

The sum of longshore sand transport owing to waves along fetch F2 and F2' is also 0 because of symmetry of wave incidence. On the other hand, because the

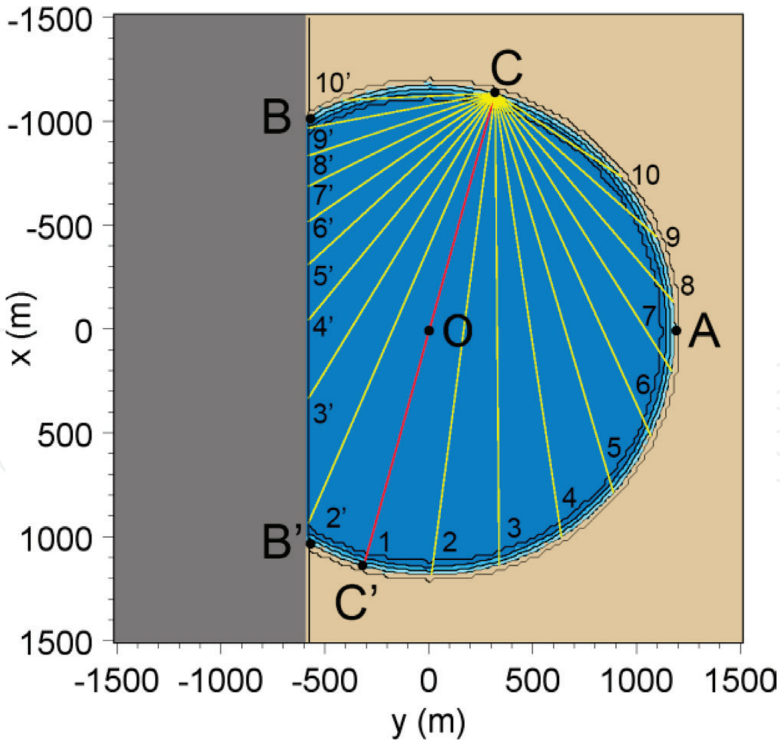

Figure 8.
Change in fetch distances owing to land reclamation.

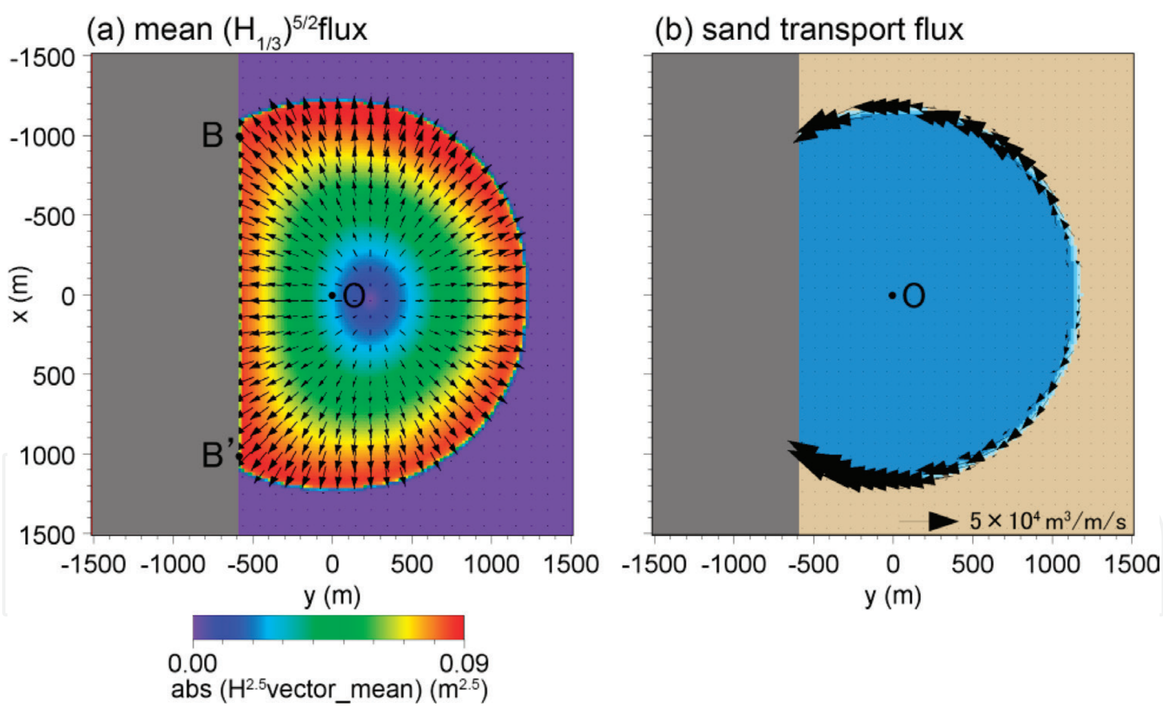

Figure 9.
Mean $(H_{1/3})^{5/2}$ flux and sand transport flux averaged over 1000 steps.

relations F3' ≤ F3, F4' ≤ F4, …, and F9' ≤ F9 are satisfied in **Figure 8**, the sum of longshore sand transport from the direction between fetch F2' and F9' is always smaller than that from the directions between fetch F2 and fetch F9. As a result, longshore sand transport toward the reclaimed land becomes larger than that toward the opposite direction at point C, resulting in shoreline recession on the opposite side of the reclaimed land and sand deposition near the reclaimed land. When the area of the water body on the left and right sides of line CC' is compared, the action of waves incident from the large water body is stronger, resulting in increase in longshore sand transport.

Mean energy flux of waves $(H_{1/3})^{5/2}$ is weak in the central part of the lake, and increases near the shoreline (**Figure 9(a)**). Moreover, along the shoreline in the upper and lower halves of the water body, waves are obliquely incident counterclockwise and clockwise to the direction normal to the shoreline, respectively. Although longshore sand transport is small on the shore opposite to the reclaimed area, it increases with the proximity to the reclaimed land (**Figure 9(b)**), and the lakeshore changes are triggered by this spatial imbalance of longshore sand transport.

4. Prediction of lakeshore changes after construction of detached breakwaters in a lake

4.1 Calculation conditions

When several detached breakwaters are constructed along the lakeshore, characteristic lakeshore changes can be seen along the lakeshore, because a lake has a closed system of littoral drift. Here, a circular lake of 1 km radius was considered, and six detached breakwaters with 400 m length and offshore distance of 400 m are assumed to be constructed in a lake. The depth of a circular water body was assumed to be 3 m, and a sandy beach with a berm height of 1 m and a uniform slope of 1/20 was set along the peripheral shoreline of a lake. Wind velocity was assumed to be 20 m/s, and wind blew from all directions with the same probability of occurrence and intensity. The wind direction in each step was set using random numbers. **Table 3** summarizes the conditions for the calculation of the lakeshore changes when detached breakwaters were constructed in a circular lake.

4.2 Calculation results

When detached breakwaters were constructed in a lake at the same time, the wave-shelter zones were formed behind the detached breakwaters, and cuspate forelands had started to be formed by 10^4 steps (**Figure 10(b)**). Up to 2×10^4 steps, the shoreline of all forelands connected to the detached breakwaters forms tombolos, as shown in **Figure 10(c)**. Finally, six pocket beaches were formed between

Calculation method	Type 6 BG model
Wind velocity	20 m/s
Berm height h_R	1 m
Depth of closure h_c	3 m
Equilibrium slope $\tan\beta_c$	1/20
Coefficients of sand transport	Longshore and cross-shore sand transport coefficient K_s = 0.2
Mesh size	$\Delta x = \Delta y = 20$ m
Time intervals	$\Delta t = 10$ h
Duration of calculation	10^6 h (10^5 steps)
Boundary conditions	Shoreward and landward ends $q_x = 0$ Right and left boundaries $q_y = 0$

Table 3.
Conditions for the calculation of the lakeshore changes when detached breakwaters were constructed in a circular lake.

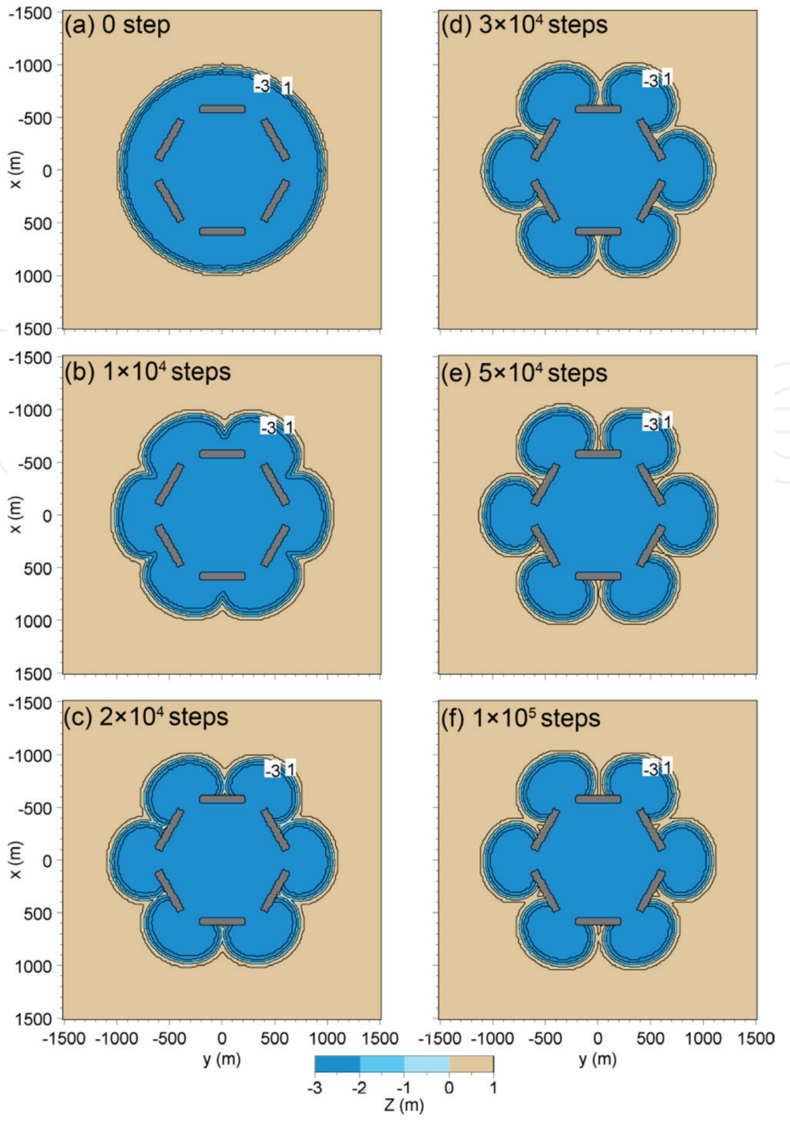

Figure 10.
Formation of cuspate forelands behind six detached breakwaters installed in a circular lake of 1 km radius.

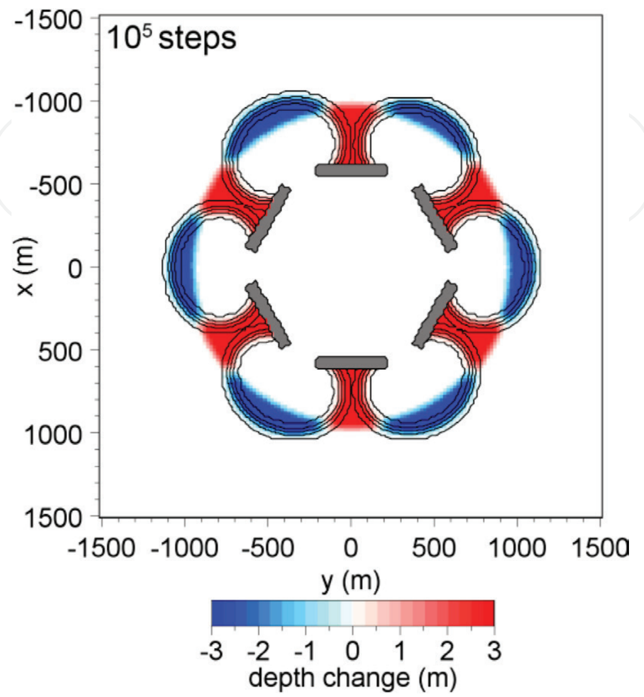

Figure 11.
Seabed difference after 10^5 steps with reference to initial topography.

detached breakwaters after 10^5 steps and stabilized, as shown in **Figure 10(f)**. **Figure 11** shows the seabed difference after 10^5 steps with reference to the initial topography. Sand deposition behind the detached breakwaters and shoreline recession in the openings of the detached breakwaters were triggered by the construction of detached breakwaters, and symmetrical topographic changes took place owing to the symmetrical arrangement of detached breakwaters.

5. Prediction of formation of oriented lakes

5.1 Examples of oriented lakes

In the Arctic Coastal Plain, typical examples of oriented lakes can be found from the satellite images [12]. **Figure 12** shows the satellite image of the coastal lowland at a location (69°13′41.66″N, 160°01′39.84″E) with an elevation of 8 m above MSL, facing the East Siberian Sea in Russia [15]. In this area, many lakes have been formed; three oriented lakes with the principal axis of the NW-SE direction can be seen 20 km west of the Kolyma River, and each lake is separated by a slender sandbar. Seaward of these lakes, many ridges extend in parallel to the shoreline, and the principal axis of these oriented lakes is in parallel to the shoreline [15]. From these characteristics, it is inferred that oriented lakes of this shape could develop, because the strength of the sea breeze is larger than that of the wind blowing from the other direction.

The second example is the oriented lakes west of Point Barrow (70°55′ 32.54″N, 157°27′ 37.11″W) in north Alaska separating the Chukchi and Beaufort Seas (**Figure 13**). In this figure, sand spits and hooked shoreline, which are assumed to have developed owing to the shoreline instability [1–3], run in the SW-NE direction. In **Figure 14**, an enlarged satellite image of the rectangular area in **Figure 13**, a number of oriented lakes can be seen with the direction of the principal axis of N7°W [15]. The direction normal

Figure 12.
Example of oriented lakes in East Siberia.

to this axis is N97°W, and wind of this direction is assumed to have a primary effect to the formation of oriented lakes. This wind direction makes a large angle of 82° to the direction of N15°W normal to the shoreline of the sand spit located at the left end in **Figure 14**. Taking into consideration the fact that wind waves are generated by wind

Figure 13.
Oriented lakes west of Point Barrow in Alaska separating Chukchi and Beaufort Seas.

Figure 14.
*Enlarged satellite image of rectangular area shown in **Figure 13**.*

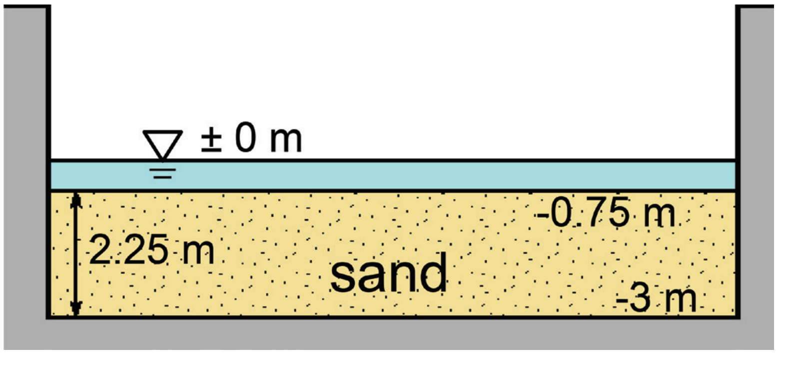

Figure 15.
Cross section of initial lake bed composed of sand.

from this direction, the shoreline instability could occur because of a large wave incidence angle. Thus, in this case, the development of oriented lakes owing to the intensive prevailing wind and the occurrence of the shoreline instability correspond well.

5.2 Calculation conditions

Assuming a shallow lake with a flat sandy bed of 0.75 m depth and the thickness of sand layer of 2.25 m as the initial topography, the development of the oriented lakes was investigated (**Figure 15**). The calculation domain was a square with 2 km length. The lake boundary was given by a solid vertical wall.

At the initial stage, infinitesimal random noise of ΔZ = 0.1 m was added to the lake bed. h_R and h_c were assumed to be 1 and 3 m, respectively. The water depth of the flat shallow lake was shallower than h_c, so that sand deposited on the flat bed at the initial stage could be quickly redistributed by wave action, leading to the formation of a sloping beach. The wind velocity was assumed to be 20 m/s, and an asymmetric (elliptic) probability distribution for the occurrence of wind direction with an aspect ratio of 4 was assumed, such that the principal axis of the probability of occurrence of wind direction was at an angle of 45° to the x-axis (**Figure 16**), although the wind was assumed to blow uniformly from all directions as described in [15], i.e., a symmetric circular distribution. Wind velocity of 20 m/s employed is the one which generates 0.8 m of significant wave height, given the wind fetch distance along the diagonal in the initial lake as 2.8 km. The conditions for the calculation of the formation of oriented lakes are summarized in **Table 4**.

5.3 Calculation results

The calculation results are shown in **Figure 17**. When wind blew obliquely to the shallow body of water of 0.75 m depth, a number of slender small lakes had emerged up to 2 × 10^3 steps, as shown in **Figure 17(b)**, via the mechanism proposed in [6]. After 5 × 10^3 steps, these slender small lakes had merged into larger lakes,

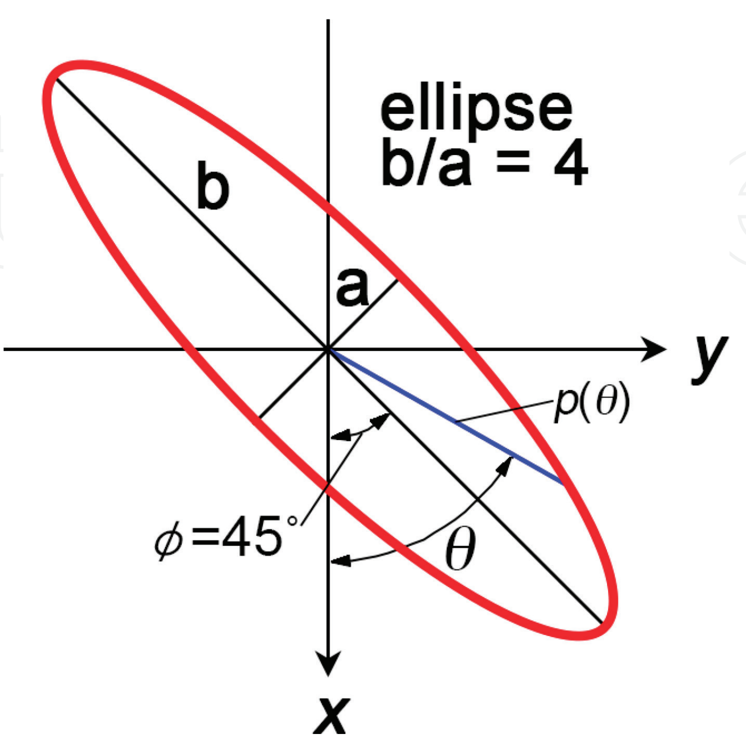

Figure 16.
Probability distribution of occurrence of wind direction.

Calculation method	Type 6 BG model
Wind velocity	20 m/s
Berm height h_R	1 m
Depth of closure h_c	3 m
Equilibrium slope $\tan\beta_c$	1/20
Coefficients of sand transport	Longshore and cross-shore sand transport coefficient K_s = 0.2
Mesh size	$\Delta x = \Delta y = 20$ m
Time intervals	$\Delta t = 5$ h
Duration of calculation	10^6 h (2×10^5 steps)
Boundary conditions	Shoreward and landward ends $q_x = 0$ Right and left boundaries $q_y = 0$

Table 4.
Conditions for calculation of formation of oriented lakes.

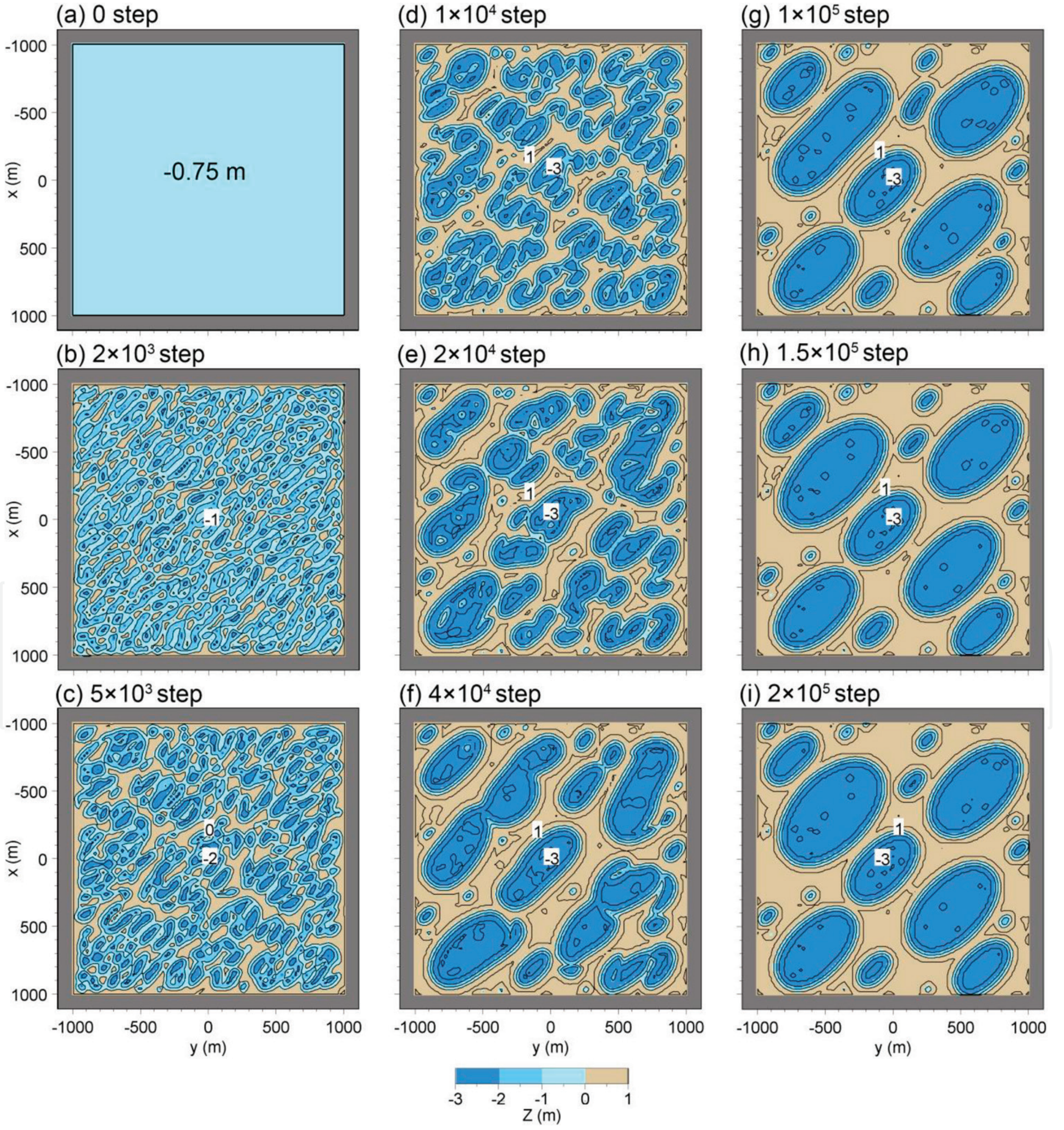

Figure 17.
Prediction of formation of oriented lakes.

and the width of the lakes increased (**Figure 17(c)**). After 10^4 steps, small lakes had further merged into larger lakes, although the shape of the oriented lakes was unclear at this stage (**Figure 17(d)**). After 2×10^4 steps, several lakes similar to the oriented lakes had developed owing to the merging of small lakes with principal axes in parallel with each other (**Figure 17(e)**). After 4×10^4 steps, oriented lakes of almost elliptic shape were formed (**Figure 17(f)**). After 10^5 steps, oriented lakes of elliptic shape were formed with a large aspect ratio (**Figure 17(g)**). It should be noted that the direction of the principal axis of the oriented lakes became normal to the direction of the principal axis of the probability distribution of occurrence of wind, as shown in (**Figure 17(g)**), and the oriented lakes reached a stable form up to 2×10^5 steps shown in (**Figure 17(i)**). The coexistence of the oriented lakes of

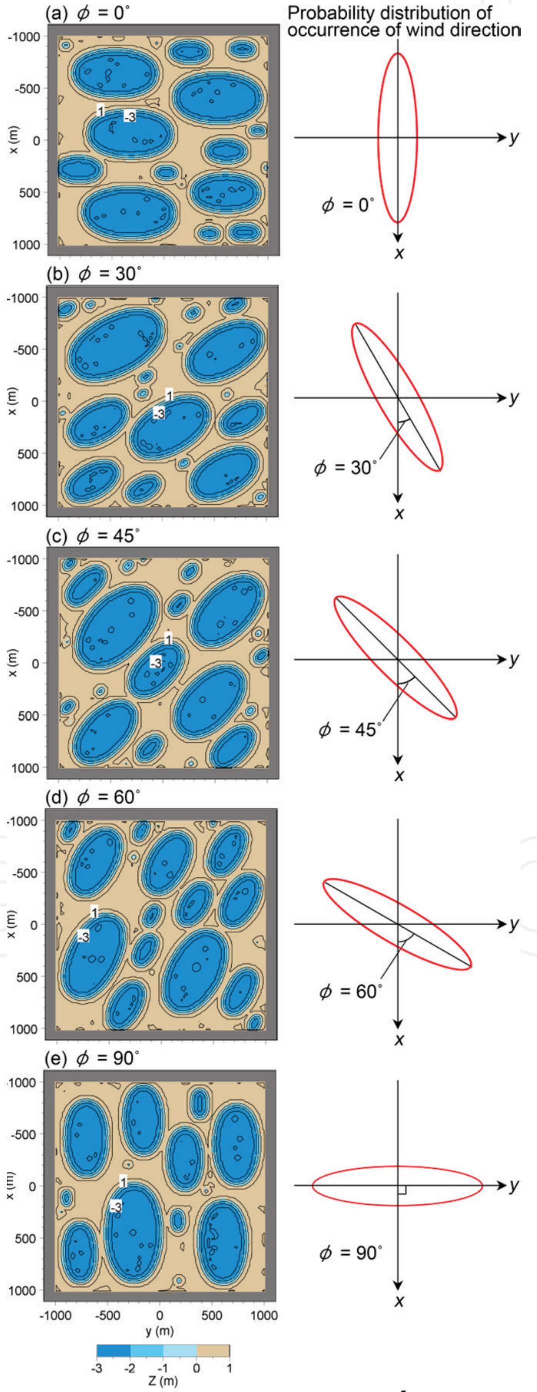

Figure 18.
Change in configuration of oriented lakes up to 2×10^5 steps in response to changes in principal wind direction.

various scales as seen in the results is found in the examples of the oriented lakes (**Figures 12–14**).

Moreover, the change in configuration of the oriented lakes in response to the change in the principal wind direction was investigated by changing the principal wind direction in five cases of Φ = 0, 30, 45, 60, and 90°. In each case, the initial condition and the other calculation conditions were maintained constant except the principal wind direction. The results of the calculation after 2×10^5 steps are shown in **Figure 18**. When the principal wind direction changed counterclockwise, the principal axis of the oriented lakes became normal to the principal wind direction, and the direction of the oriented lakes always became normal to the principal wind direction, as shown in **Figure 18(a)–18(e)**.

6. Conclusions

In Chapter 8, three topics were discussed, and topographic changes were predicted using the Type 6 BG model: (1) 3D segmentation of elongated water body, (2) deformation of a circular lake by wind waves when a straight seawall cutting a part of the water body was constructed or detached breakwaters were constructed in a lake, and (3) prediction of formation of oriented lakes:

1. In a slender water body with a large aspect ratio, the angle between the direction normal to the shoreline and the wave direction exceeds 45° because of a long wind fetch distance along the principal axis, resulting in the emerging of cuspate forelands and the subdivision of a water body. The Type 6 BG model was used to predict such changes in a water body. The calculated results were compared with the ones observed in a water body facing Chukchi Sea and Lake Kitaura, and the 3D subdivision process of a long slender water body was successfully explained.

2. Lakeshore changes triggered by artificial alteration were predicted. When a straight seawall cutting off a circular lake was constructed, the center of the rounded lake approached the seawall, causing the shoreline recession on the opposite shore against the seawall, suggesting that the land reclamation on part of a lake should be careful. Also, the impact of the construction of six detached breakwaters in a lake was investigated. After the construction, lakeshore was subdivided into six pocket beaches fixed by detached breakwaters.

3. When wind blew uniformly from all directions over a water body, a lake with a highly circular shape was formed [6]. In contrast, the shape of the lakes became elliptic when wind blew with an asymmetric probability distribution of occurrence of the wind direction. Thus, the formation of oriented lakes was successfully explained using the Type 6 BG model, and the predicted results and the examples given in [12] were in good agreement. The calculation results clearly indicate that the direction of the principal axis of the oriented lakes became normal to the direction of the principal axis of the probability distribution of occurrence of wind.

Author details

Takaaki Uda[1]*, Masumi Serizawa[2] and Shiho Miyahara[2]

1 Public Works Research Center, Tokyo, Japan

2 Coastal Engineering Laboratory Co., Ltd., Tokyo, Japan

*Address all correspondence to: uda@pwrc.or.jp

References

[1] Ashton A, Murray AB, Arnault O. Formation of coastline features by large-scale instabilities induced by high angle waves. Nature. 2001;**414**:296-300

[2] Ashton A, Murray AB. High-angle wave instability and emergent shoreline shapes: 1. Modeling of sand waves, flying spits, and capes. Journal of Geophysical Research. 2006;**111**:F04011. DOI: 10.1029/2005JF000422

[3] van den Berg N, Falqués A, Ribasz F. Long-term evolution of nourished beaches under high angle wave conditions. Journal of Marine Systems. 2011;**88**(1):102-112

[4] Zenkovich VP. Processes of Coastal Development. New York: Interscience Publishers, Div. of John Wiley and Sons, Inc; 1967. p. 751

[5] Ashton A, Murray AB, Littlewood R, Lewis DA, Hong P. Fetch limited self-organization of elongate water bodies. Geology. 2009;**37**:187-190

[6] Uda T, Serizawa M, Miyahara S, San-nami T. Prediction of segmentation and mergence of shallow water bodies by wind waves using BG model. In: Proc. Coastal Dynamics 2013, Paper No. 166. 2013. pp. 1729-1740

[7] Uda T, Serizawa M, Miyahara S. Numerical simulation of three-dimensional segmentation of elongated water body using BG model. In: Proc. 33rd ICCE, Sediment. 65. 2012. pp. 1-11. https://icce-ojs-tamu.tdl.org/icce/index.php/icce/article/view/6533/pdf_448

[8] Serizawa M, Uda T, Miyahara S. Prediction of development of sand spits and cuspate forelands with rhythmic shapes caused by shoreline instability using BG model. In: Proc. 33rd ICCE, Sediment. 35. 2012. pp. 1-11. https://icce-ojs-tamu.tdl.org/icce/index.php/icce/article/view/6534/pdf_534

[9] Serizawa M, Uda T, Miyahara S. Segmentation of water body given probability of occurrence of wind direction by circular or elliptic distribution. In: Proc. 35th Inter. Conf. Coastal Eng., Sediment. 6. 2016. pp. 1-15. https://icce-ojs-tamu.tdl.org/icce/index.php/icce/article/view/8104/pdf

[10] Uda T, Serizawa M, Miyahara S. Segmentation of water body and lakeshore changes behind an island owing to wind waves, Chap. 4. In: Malcangio D, editor. Applications in Water Systems Management and Modeling. Rijeka: IntechOpen; 2018. pp. 49-70. 129 p. https://www.intechopen.com/books/applications-in-water-systems-management-and-modeling/segmentation-of-water-body-and-lakeshore-changes-behind-an-island-owing-to-wind-waves

[11] Serizawa M, Uda T, Miyahara S. Effects of construction of offshore breakwaters on segmentation of a slender water body. In: 8th Int. Conf. on Asian and Pacific Coasts (APAC 2015), Procedia Engineering. Vol. 116. 2015. pp. 502-509

[12] Seppälä M. Wind as a Geomorphic Agent in Cold Climates. Cambridge University Press; 2004. p. 358

[13] Harry DG, French HM. The orientation and evolution of thaw lakes, southwest Banks Island, Canadian Arctic. In: Proceedings, Fourth International Conference on Permafrost. Washington, D. C: Natl. Acad. of Sci; 1983. pp. 456-461

[14] Mackay JR. The Mackenzie Delta Area, N.W.T. Vol. 8. Ottawa, Memoir: Geographical Branch, Mines and Technical Surveys; 1963. 202 p

[15] Uda T, Serizawa M, San-nami T, Miyahara S. Prediction of formation of oriented lakes. In: Proc. 34th ICCE. 2014. pp. 1-12. https://journals.tdl.org/icce/index.php/icce/article/view/7109/pdf_413